

أشكال مستشعرات الألياف الضوئية وتطبيقاتها:

تصميم الألياف متعددة الأنوية

م.م بتول علي عريان

مديرية تربية واسط

ملخص

يُعد مستشعر الألياف الضوئية المُشكّل تقنية استشعار موزعة تُحدد انحناء ومعدل التواء هيكل مُعين باستخدام إشارات مُشتتة من ليف متعدد الأنوية. تُنقل المعلومات عبر الألياف الضوئية عن طريق تعديل الإشارات الضوئية، عادةً باستخدام الليزر أو المواد المُصدرة للضوء. من خلال الحل العددي لمجموعة مُحددة من المعادلات والبرامج ثلاثية الأبعاد، يتم تحديد هندسة الألياف الضوئية متعددة الأنوية. تتميز التقنية المُقدمة بتحديد الأبعاد الثلاثية المُعقدة، وعلى عكس حل الحدود المُتكاملة في التقنيات السابقة، حيث تُشكل الألياف كحل مُستمر ولها انحناءات مُميزة في مستوى واحد. النتائج وتحليل أخطاء التقنية، استُخدمت الألياف الضوئية ثلاثية الأنوية لأول مرة. وُجد أن نسبة طول الألياف في هذا البحث تبلغ ٦.٩%. وقد أُتيحَت مؤخرًا طريقة مُبتكرة لفك تشفير كابل ألياف ضوئية مُتعدد الأنوية. باستخدام قيم مميزة للحمل المُكتسب في كل مركز، تُنشئ هذه الطريقة صورة ثابتة للانحناء مع انحناء في الألياف. يهدف المزيد من العمل إلى القضاء تمامًا على هذا الخطأ، بما في ذلك خصائص الالتواء.

Abstract

Optical fiber shaped sensor is a distributed sensing technique that determines the curvature and twist rate of a given structure by utilizing scattered signals from a multi-core fiber, information is transmitted across optical fibers by altering light signals, usually with the use of lasers or light-emitting. Through the numerical solution of a given set of equations and programs in three dimensions, the geometry of a multicore optical fiber is determined. The presented technique is characterized by defining complex three-dimensionality, and unlike the integrated boundary solution in previous techniques, where the fibers are formed as a continuous solution and have distinct curvatures in one plane. Outcomes and technique error analysis three-core optical fiber is used for the first time. The proportion of fiber length in this investigation was found to be 6.9%. An innovative method for deciphering a fiber-optic cable with many cores configuration was recently made available. Using distinct values of load acquired in every center, the method creates a constant image of bending with curving in fibers. Further work aiming at fully eliminating this mistake made by include characteristics of twisting.

1. Introduction

Since 1990s optoelectronics and fiber optics technology underwent significant advances due to innovations in the telecommunications, semiconductor and consumer electronics sectors (R. Kashyap 2010). The developments of compact disk (CD) players, laser printers and the high performance and reliable optical fiber communication are the result of these advances (M. J. Gander et al. 200). The optical fiber sensor technology is a direct outgrowth of the revolutions taken place in optoelectronics and fiber optic communication industries. Many of the components associated with these industries are used for optical fiber sensor applications. In the beginning the main hurdle in the development of sensors was the cost of components such as optical sources and detectors (G. M. H. Flockhart et al. 2003, B. A. Childers et al. 2001). With the time, components prices are falling and the improvements in fiber, laser and photodetector technology have taken place. It is expected that as the time progresses the optical fiber sensors will replace the conventional devices for the measurements of various physical, chemical and biological parameters such as rotation, acceleration, electric and magnetic fields, temperature, pressure, acoustics, vibration, position, strain, humidity, viscosity, pH, glucose, heavy metals, gases, viral infection, pollutants etc (R. G. Duncan et al. 2007, Herbers M et al. 2003).

Optical fiber sensor technology is an extremely promising and fast growing technology. At present there are about 100 companies with optical fiber sensor products available and 150 with products in development. It shows the utility of the technology and acts as a thrust for further development in this field (S. M. Klute et al. 2006). The current market for optical fiber sensor systems has been reported to be in the region of \$650 million. The global market for sensors is expected to reach more than \$70 billion by 2030. In a fiber optic sensor the heart of the sensor is an optical fiber. An optical fiber in its simplest form is a cylindrical symmetric structure consisting of a central 'core' glass/plastic of uniform refractive index and of diameter 4-600 μm (A. Gray 1993). It is surrounded by a 'cladding' glass/plastic of slightly lower refractive index. To provide the mechanical and environmental protection to the fiber, the cladding is covered with an external plastic coating as in Fig.1. The light in the fiber propagates by bouncing back and forth from the core-cladding interface. The design of the fiber optic sensor depends critically on the choice of optical fiber (J. Langer and D. A. Singer 1996). Telecommunication fibers are inexpensive but may not be the right choice for sensors. Some of the fiber optic sensors dictate the

use of application-specific optical fibers. In this chapter we shall first describe ray analysis for the light propagation in the fiber. The modes propagation, numerical aperture of the fiber, fiber characteristics and different kinds of optical fibers used for sensing will be described later (C. de Boor 2001).

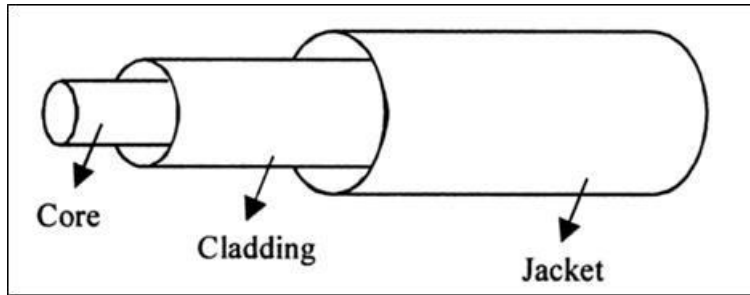


Figure.1.Geometry of an optical fiber

The objective of preparing this study is to introduce a new innovation to the engineering of multi-core optical fibers using numerical methods and three-dimensional (3D) modeling, and to provide a model that surpasses previous methods by providing a more accurate, efficient, and continuous solution to the shape of the fiber, especially with regard to complex three-dimensional bends. The scientific contribution of the current study lies in developing the numerical solution and 3D modeling technology for multi-core optical fiber engineering, as well as improving previous methods by providing appropriate solutions and processing of complex 3D bends, and working to apply this technology to all three-core optical fibers. In addition, the study provides an analysis of technical error, which gives us a better understanding of the accuracy of the work and a distinct vision for future improvements.

2. Generic Optical Fiber Sensor

A schematic architecture of a typical optics fiber detector as in Fig.2, A source of brightness is necessary to operate the sensor's simple monitoring, method of identification, scheme of reference, and sensing design. Photodetector.1 is utilized as a reference in the diagram since it is used to verify the fluctuations in the lamp's power supply. Appropriate optics are used to couple the rays of the point of origin into the cable. The fiber's exterior or interior can be where of the detecting action (Bado MF et al. 2021). Similar or alternative optics can be used to convey the shift in energy output caused by the measurement. The change in output power is detected by the photodetector 2. Both basic and elaborate equipment are possible. According to the specific use. The features of the gadget, including its ability to sense and range of motion, are largely dependent on the selection of the beam

location, optical fiber properties, and sensing mechanism. For instance, the acceptable range of frequencies depends on the fiber's composition (Howiacki T et al. 2023). Given that the sensor's ability to function depends on important parts such fiber optics, both the sensor and the power source Understanding the fundamentals of optics and the properties of supplies and detection that are available and may be employed in the creation of optical sensors is crucial.

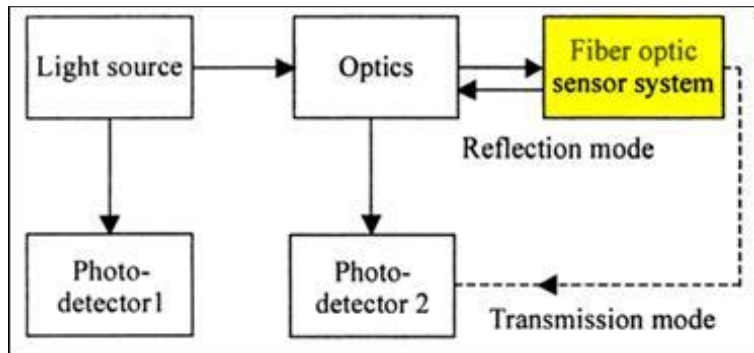


Fig. 2. Block diagram of a generic optical fiber sensor

3. Fields of Applications

Optical fiber sensors are finding their way into an ever-increasing number of applications as scientists, engineers and designers take advantage of their unique abilities. Their applications in some of the fields are described below:

3.1 Pollution monitoring (sea, water and air): Optical fiber sensors can be used to detect a large number of toxic substances and other chemical constituents such as formaldehyde, ammonia, nitrogen oxides, chloroform, hydrogen sulfide, sulfur dioxide, hydrocarbons etc. in sea, water and air. The main advantage of optical fiber sensors is rapid in situ measurement and remote sensing (Buda-Ozog L et al. 2022). Since the signal is optical rather than electrical, there will not be any electrical interference that are normally present in a typical shipboard environment.

3.2 Buildings: Optical fiber sensors also find application in structural monitoring. By measuring stress and strain in bridges, buildings, dams and tunnels - where failure can mean disaster-these sensors provide crucial analysis. The sensors are small enough to be embedded into the structure of buildings or vehicles and therefore can monitor passively and continuously the structure, providing information that can be tracked over time to indicate important structural changes (Bassil A. et al. 2020). These sensors can provide early warning of weaknesses in structure so that minor repairs can be made before major disaster strikes. In petroleum engineering, for example,

these sensors are used for remote monitoring of the structure and function of an oil well to prevent hazards or malfunction. As the search for oil intensifies, wells are being drilled deeper, and monitoring equipment faces great demands in terms of pressure and temperature. Optical fiber sensors are also being used in squeezing the last ounce of production from old oil wells by optimizing the amount of water or steam injection used to efficiently remove reserves.

- 3.3 Biomedical sciences:** The greatest field of application is sensing clinically and biochemically important analytes. Accurate and rapid measurement of the level of these analytes in blood are critical to good medical practice and patient care. To measure, blood samples are withdrawn from the patient and sent to the clinical laboratory to determine their contents. The delays and potential errors that can be introduced because the laboratory is far from the patient and from the physician who interprets the test results, may cause therapeutic decisions to be made without adequate information (Zhang S et al. 2021). If a large number of measurements are to be made per day then withdrawing sample and taking to the laboratory each time is not practical. Further, elderly, critically ill, or very small patients simply cannot afford to lose any blood. Fiber optic sensors with miniaturized probe can overcome these problems.
- 3.4 Biotechnology:** The main problem with conventional electrodes or electrode-based biosensors is the sterilization. The measurement of physical and chemical parameters in bioreactors requires sterilized sensors (Zdanowicz K et al. 2022). For optical fiber sensors, sterilization is not a problem. The fibers can be sterilized by steam at 115- 130°C without compromising their performance. Thus optical fibers can be used in sensing O₂, pH, PCO₂, glucose, glutamate in fermentation plants.
- 3.5 Ground water monitoring:** Because of public concern about the quality of drinking water, continuous monitoring of ground water has become a necessity. By introducing fibers down to the ground water level one can monitor the pH of the water and the amount of chloride, uranium, organic pollutants and tracer substances present in water before digging a well. This will save drilling cost because fibers hold (1-2 cm diameter) allows the use of small bare-holes. Further, using optical fibers the quality of the water can be monitored in situ and in real time (Deutscher Beton- und Bautechnik-Verein

2018). Thus, there will not be any need to take sample and get it analysed in laboratory.

3.6 Process control: Production efficiency and product quality depend on process control. The optical fiber sensors can do on- line measurements and that in factory itself. Further there is no risk of fire/spark in the factory due to fiber sensors. Another advantage is they can be used in explosive environment (Novak B et al. 2021). During process temperature, pressure, flow, liquid level, analytical parameters etc can be measured with optical fiber sensors.

3.7 Titrimetry: The optical fibers can be used in various titrimetric procedures including acid-base titrations, argentometry, bromometry and iodometry, complexometry, or redox titrations. The advantage is less cost because electrodes are expensive (Luna Innovations Inc 2022).

3.8 Military/Aerospace: Optical fibers can be used in gyroscope for rotation measurement, flight controls, engine monitoring, nuclear radiation testing, security systems etc. (O'Haver T. 2022).

4. Material and method

4.1 Fiber Bending

This work concentrates on the instance of neatly oriented tri-core cable, which requires the measurement of at least three distinct core stresses being able to determine the three-dimensional curving length along with the angle of bent. The standard tri-core straight fiber's cross-sectional configuration is shown in Figure 3.

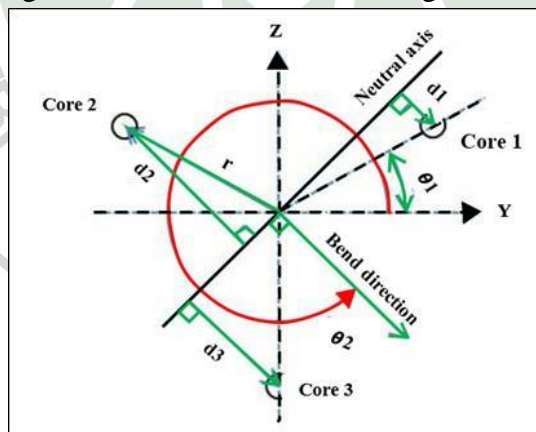


Fig. 3. Circuit for the stress resulting from bending

$2\pi/3$ distance with a radius displacement of r to the middle, with θ_1 denoting core.1 offset from $\theta = 0$ axis, determine where the centers are located inside fiber's

sectional view. Fiber coating and cladding boundaries are not visible in Fig.3. As previously mentioned, θ_1 determines its centers' alignment with respect onto the fabric structure that holds the fibers and is presumed to remain constant throughout the fiber. Usually, the straightforward calibration approach of twisting the material in an angle that exists, calculating individual centers' strain coefficients, and calculating a number derived using the bent planes with the collected strain readings knowledge is used to set the value of θ_1 .

To clarify the process of twisting while curling of 3D arcs defined by the material fibers, initially, suppose if it functions as straight, it has a homogeneous volume with an annular sections because it is equal. The carbon fibers structure's link to an organic curving structure that it lies along can be simply defined as a result of this assumption. The link across the fibers will remain consistent across the organic curved framework with the substance of the fibers structure if it is free-sleeved, which means it lives within a perfect, smooth restriction that is completely simply one side is fastened. Slaving fabric freely allows for the material is worked into complicated shapes in the context form detection using multi-core fibers without introducing outside forces that bend fibers. Additionally, according to this setup, all derived torsion was the outcome from the fiber's random form or curving, and ensuring that each fiber's length is consistent to the centers' angle alignment during its length zero.

4.2 Engineering Equations for Arbitrary Bending

The hypothesis of the study states that light propagating in an optical fiber follows a helical path due to the existence of a fiber refractive index gradient, curvature and torsion of the curve, which can be related to the helical path followed by light in an optical fiber. The tangent vector represents the direction of light propagation, the principal normal vector represents the curvature of the fiber, and the dual vector represents the helical twist of the fiber. Fiber bending and twisting also affect propagation properties, such as mode coupling, dispersion, and loss.

Therefore, the following formulas provide a mathematical framework for understanding and analyzing the curved paths of light in optical fibers, which is relevant to the study and design of optical fiber communications systems.

$$\Delta\varepsilon = \frac{d}{R} = \frac{d^2}{R} \dots\dots\dots (1)$$

$\Delta\varepsilon$ = strain values

R = bent radius for the optic

d = the separation from two bent axis optic centers

$$\varepsilon_i = -kr \cos\left(\theta_b - \frac{2\pi}{3} - \theta_i\right) \dots\dots\dots (2)$$

ε_i = axial strain in the core

r = distance from the core to center of fiber

θ_b = angular offset from the local y-axis to the fiber bending direction

θ_i = angular offset from the local y-axis to the core.

Even though the results from a symmetric it focuses on tri-core fibers, eq.2 can be applied to any number of cores arranged in any way, whether symmetric or asymmetric. Curvature has previously been calculated and contrasting the pressure data between two sets of circuits. Large curvature inaccuracies can result from strain measurement inaccuracy, despite the mathematical sufficiency of this procedure. In order to minimize inaccuracy with one estimate of load and compute curvature utilizing data from all cores, first create a direction of perceived bending that highlights taken from fiber's center toward the core:

$$k = \frac{2\sqrt{(\sum \varepsilon_i \cos \theta_i)^2 + (\sum \varepsilon_i \sin \theta_i)^2}}{N r} \dots\dots\dots (3)$$

N = the amount of optic strands

The computations of equations (2, 3) it happens for each triplets in the F.B.G through the fabric to produce distinct bending groups, and curve in the path, in particular places, of the material that corresponds to F.B.G.

4.3 Data Made Experimentally

Eight distinct shapes were used to put a tri-core straight fibers with a circumferential center length of sixty-eight μm , diameter of covering 300 μm , in blueprints, 520 μm covered size. Panels with cylinder an elevated density were CNC machined to create grooves, which served as the templates. The fabric was supplied via a fibreglass ring with twenty gauge, which was inserted into the furrows of the models and secured placed in position, to minimize the fiber's and the template's contact.

Rayleigh grids are paired with every core of the fiber at intervals of 10 mm. An optic spectrum reflectometer with 3 channels (O.F.D.R) framework was used to measure the grating wavelengths, relative base frequencies of gratings were established as the cable was being secured simple. Taking use of a straining for each wavelength relation of $750.6 \mu\text{e}/\Delta\text{nm}$ shift, the wavelength information was transformed into varietal information, which was then worked to produce solution like earlier mentioned.

The known curve coordinates are subtracted from the measured form to determine the observed shape error. An item containing 5 machine-made ridges along the

outside serves as the initial template. The grooves, identified as P1 through P5, have greatest bends between 15 and 75 meter⁻¹, and they conform to planar curves with a total arc length of 84 cm. There is an area with zero bending along the optic, one flex, and zero bending along the optic due to the grooves' placement on the surface. A 0.6 m long pattern was the additional one, 0.12 m radius cylindrical with 3 carved slots (C.1, C.2, and C.3) superficially.

Curves C1, C2, and C3 have arc-lengths of 1.03, 1.11, and 1.68 meters, in that order. Parametric curves with a constant radius in cylindrical dimensions define the grooves. Figures 4(a) display the Z- θ connections for the reference arcs in both two and three dimensions, respectively, while Figure 4(b) depicts an illustration in three dimensions of form C.1.

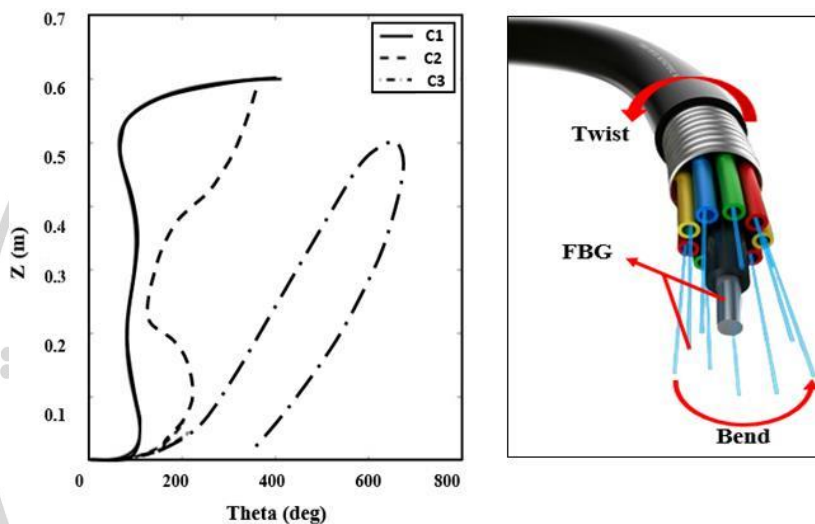


Figure. 4(a) Z- θ relationships. (b) Three-dimensional representation C.1

5. Results

Figure.5 displays the absolute measured shape error as well to be the inaccuracy for measurement of the flat arcs at any filtering a trio. P.1-5. The planar configurations' maximum error per unit length, or 1.68%, is found in a bend P.3, where a 7.06 mm error occurs at 0.39 m down the fabric. Main causes of the defects there are variations on the curved line in forms P.1-P.5., which are probably brought on with bent weights that the fiberglass sleeve applies to the fiber during its deformation under tight bends.

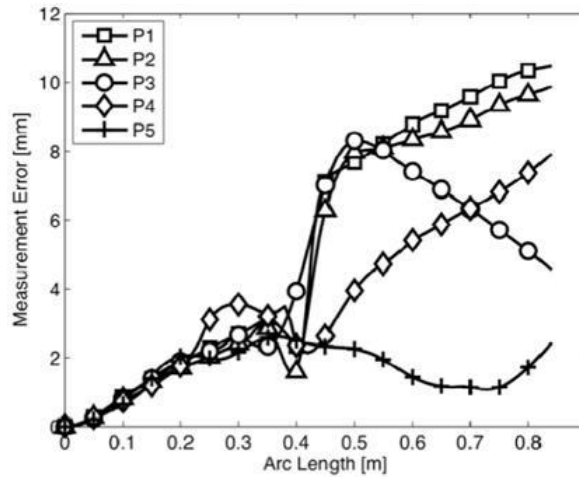


Figure.5 Measure errors in absolute value (P)

Figure.6 displays the absolute observed form error as well as the mistake for each filtering a triplet for each duration for curving in three dimensions C.1–C.3. In the three-dimensional configurations, the maximum error per unit length is 6.99%; curve C.2 exhibits this error with a 33.01 mm inaccuracy at 0.52 m throughout the fabric. Like in the linear examples, the mistake is probably caused by twisting loads being applied to the fiber by the fiberglass sleeve. Table.1 displays the the cubic root of average, greatest absolute, highest %, and last mistakes for every form.

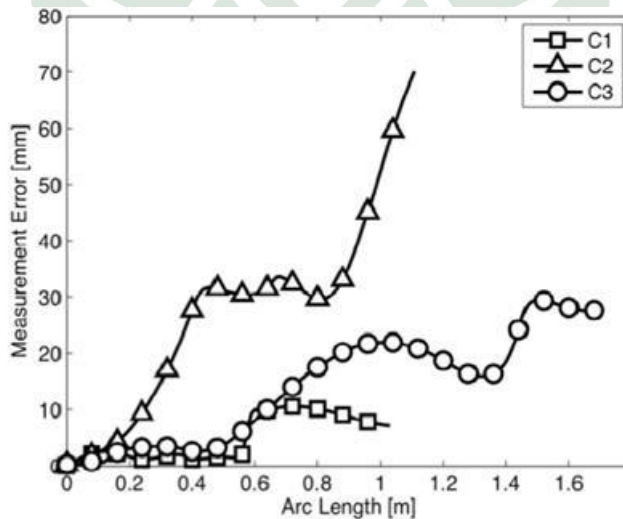


Figure.6. Measure errors in absolute value (C)

Table 1. Stats Fault Data

Description	P.1	P.2	P.3	P.4	P.5	C.1	C.2	C.3
Length Fiber in meter	0.82	0.82	0.82	0.82	0.82	1.02	1.12	1.57
R.M.S.E (mm)	4.66	6.32	6.63	5.76	3.56	6.23	33.42	16.82
Error Max (mm)	9.43	10.85	10.73	9.15	5.69	10.46	70.14	29.36
Error Max (%)	1.43	1.57	1.52	1.14	1.15	3.21	7.14	2.25
Last Error in (mm)	4.74	4.13	5.54	4.84	2.54	6.32	69.32	30.25

6. Conclusion

A novel approach to figuring out the configuration of an optical fiber cable with many cores introduced. The technique generates an ongoing picture of twisting and bending in fibers from discrete measure of force taken throughout every core. Maximum inaccuracy in shape measurements was found to be 6.9%. Most likely, twisting in the fiber caused by external forces is the main source of inaccuracy. The goal of future research will be to completely eliminate this inaccuracy by adding twist measurements to the shape solution.

One study suggested a strain analysis-based method for measuring the shape of fiber optic cables. They used strain measurements at discrete points along the cable to estimate its curvature and torsion. The accuracy of shape measurements was reported to have an error of 9.5%. However, the study did not address externally induced twisting as a source of error. The new method presented in the current study improves upon the accuracy of shape measurements, achieving an error of at most 6.9%. The primary source of error identified in the new method is externally induced twisting, which was not specifically addressed (Deutscher Beton- und Bautechnik-Verein 2018, Buda-Ozog L et al. 2022).

In another study focused on estimating the curvature and torsion of multi-core fiber optic cables using fiber Bragg gratings (F.B.G.s). By analyzing the strain changes in the F.B.G.s, they were able to calculate the shape parameters. The reported error in shape measurements was approximately 6.8%. However, the study did not discuss the incorporation of twist measurements into the shape solution. The new method presented in the current study achieves similar accuracy levels in shape measurements (6.9% error). However, the proposed method differs

by utilizing discrete strain measurements in each core rather than FBGs. Additionally, the new method acknowledges the need to incorporate twist measurements to eliminate the primary source of error (G. M. H. Flockhart et al. 2003, B. A. Childers et al. 2001).

Researchers suggested in a recent study a method based on optical frequency domain reflectometry (OFDR) for shape sensing in multi-core fiber optic cables. By analyzing the backscattered light along the cable, they estimated its shape with an error of approximately 8.3%. The study did not explicitly mention the impact of externally induced twisting. The new method presented in the current study achieves lower error rates (6.9% maximum error) compared to the OFDR-based method (8.3% error). Furthermore, the new method acknowledges the need to incorporate twist measurements to mitigate the primary source of error (R. G. Duncan et al. 2007, Herbers M et al. 2003).

References

1. A. Gray, Modern Differential Geometry of Curves and Surfaces (CRC Press, 1993), Chap. 7.
2. B. A. Childers, M. E. Froggatt, S. G. Allison, T. C. Moore, D. A. Hare, C. F. Batten, and D. C. Jegley, "Use of 3000 Bragg grating strain sensors distributed on four eight-meter optical fibers during static load tests of a composite structure," Proc. SPIE 4332, 133–142 (2001).
3. Bado MF, Casas JR, Gomez J. Post-processing algorithms for distributed optical fiber sensing in structural health monitoring applications. Struct Health Monitor. 2021;20(2):661–80. <https://doi.org/10.1177/1475921720921559>
4. Bassil A, Chapeleau X, Leduc D, Abraham O. Concrete crack monitoring using a novel strain transfer model for distributed fiber optics sensors. Sensors (Basel, Switzerland). 2020;20(8): 2220. <https://doi.org/10.3390/s20082220>
5. Buda-Ozog L, Zieba J, Sie nkowska K, et al. Distributed fibre optic sensing: reinforcement yielding strains and crack detection in concrete slab during column failure simulation. Measurement. 2022; 195:111192. <https://doi.org/10.1016/j.measurement.2022.111192>
6. C. de Boor, A Practical Guide to Splines (Springer-Verlag, 2001), Chap. 14.
7. Deutscher Beton- und Bautechnik-Verein e. V. Brückenmonitoring: Planung, Ausschreibung und Umsetzung. Berlin: Deutscher Beton- und Bautechnik-Verein e. V; 2018.

8. G. M. H. Flockhart, W. N. MacPherson, J. S. Barton, J. D. C. Jones, L. Zhang, and I. Bennion, "Two-axis bend measurement with Bragg gratings in multicore optical fiber," *Opt. Lett.* 28(6), 387-389 (2003).
9. Herbers M, Richter B, Gebauer D, Claßen M, Marx S. Crack monitoring on concrete structures—comparison of various distributed fiber optic sensors with digital image correlation method. *Structural Concrete.* 2023; 24:6123-40. <https://doi.org/10.1002/suco.202300062>.
10. Howiacki T, Sienko R, Bednarski Ł, Zuziak K. Crack shape coefficient: comparison between different DFOS tools embedded for crack monitoring in concrete. *Sensors.* 2023;23(2):566. <https://doi.org/10.3390/s23020566>
11. J. Langer and D. A. Singer, "Lagrangian aspects of the Kirchhoff elastic rod," *SIAM Rev.* 38(4), 605-618 (1996).
12. Luna Innovations Inc. Optical Distributed Sensor Interrogator Model ODiSI 6: User's Guide ODiSI 6 Software. Roanoke, Virginia: Luna Innovations Inc. 2020.
13. Luna Innovations Inc. User's Guide ODiSI-B: Optical Distributed Sensor Interrogator Model ODiSI-B: User's Guide ODiSI-B Software 5.2.0. Roanoke, Virginia: Luna Innovations Inc. 2022.
14. M. J. Gander, W. N. MacPherson, R. McBride, J. D. C. Jones, L. Zhang, I. Bennion, P. M. Blanchard, J. G. Burnett, and A. H. Greenaway, "Bend measurement using Bragg gratings in multi-core fiber," *Electron. Lett.* 36(2), 120-121 (2000).
15. Novak B, Stein F, Reinhard J, Dudonu A. Einsatz kontinuierlicher faseroptischer Sensoren zum Monitoring von Bestandsbrücken. *Beton-Und Stahlbetonbau.* 2021;116(10):718-26. <https://doi.org/10.1002/best.202100070>
16. O'Haver T. Pragmatic introduction to signal processing: applications in scientific measurement: an illustrated handbook with free software and spreadsheet templates to download. College Park, Maryland: Kindle Direct Publishing. <https://terpconnect.umd.edu/%7Etoh/spectrum/IntroToSignalProcessing2022.pdf>; 2022.
17. R. G. Duncan, M. E. Froggatt, S. T. Kreger, R. J. Seeley, D. K. Gifford, A. K. Sang, and M. S. Wolfe, "Highaccuracy fiber-optic shape sensing," *Proc. SPIE* 6530, 65301S, 65301S-11 (2007).
18. R. Kashyap, *Fiber Bragg Gratings*, 2nd ed. (Elsevier, 2010).
19. S. M. Klute, R. G. Duncan, R. S. Fielder, G. W. Butler, J. H. Mabe, A. K. Sang, R. J. Seeley, and M. T. Raum, "Fiber-optic shape sensing and

- distributed strain measurements on a morphing chevron,” in Proceedings of the 44th AIAA Aerospace Sciences Meeting and Exhibit (Reno, Nevada, Jan. 9–12, 2006).
20. Zdanowicz K, Gebauer D, Koschemann M, Speck K, Steinbock O, Beckmann B, et al. Distributed fiber optic sensors for measuring strains of concrete, steel, and textile reinforcement: possible fields of application. *Struct Concr.* 2022;23: 3367–82. <https://doi.org/10.1002/suco.202100689>
21. Zhang S, Liu H, Coulibaly AAS, DeJong M. Fiber optic sensing of concrete cracking and rebar deformation using several types of cable. *Struct Control Health Monit.* 2021;28(2):e2664. <https://doi.org/10.1002/stc.2664>

